pH-Dependent Structure and Properties of TiO_2/SiO_2 Nanoparticle Multilayer Thin Films

Daeyeon Lee,[†] Damali Omolade,[‡] Robert E. Cohen,*[,†] and Michael F. Rubner*[,‡]

Department of Chemical Engineering, Department of Materials Science and Engineering, and Center for Materials Science and Engineering, Massachusetts Institute of Technology, 77 Massachusetts Avenue, Cambridge, Massachusetts 02139

Received January 12, 2007

We demonstrate that the structure and properties of layer-by-layer assembled multilayer thin films comprising positively charged TiO_2 and negatively charged SiO_2 nanoparticles can be varied by controlling assembly conditions. The average incremental thickness of the all-nanoparticle thin films after a pair of 7 nm TiO_2 and 22 nm SiO_2 nanoparticle adsorption steps was strongly dependent on the pH of each nanoparticle suspension, varying from a few nanometers to 30 nm. The surface charge density of the adsorbing nanoparticles and that of the previously adsorbed nanoparticle layers are the crucial factors in determining the average bilayer thickness of the films. Zeta-potential measurements of polystyrene microspheres coated with TiO_2/SiO_2 nanoparticle multilayers indicated that incomplete charge reversal after the deposition of nanoparticles leads to a very small thickness increase at each adsorption step, whereas complete charge reversal results in significantly larger thickness increments. Other film characteristics including refractive index, porosity, and chemical composition of the multilayers also depended on assembly conditions but to a much lesser extent compared to the dependence observed for average bilayer thickness.

Introduction

The formation of thin films containing nanoparticles can lead to novel applications in the areas of photonics, catalysis, electronics, magnetism, and biomedical engineering.[1] Despite the recent advances in creating various types of functional nanoparticles,[2−4] it still remains a challenge to create conformal thin films of nanoparticles with precise control over the physicochemical properties. One approach that has been widely used is the layer-by-layer (LbL) deposition[5] of charged nanoparticles in conjunction with an oppositely charged polyelectrolyte.[6−16] Properties of nanoparticle-containing multilayers can be precisely tuned by controlling the assembly conditions (e.g., salt concentration and pH conditions) and the types of nanoparticles and polyelectrolytes assembled. Nanoparticle-containing multilayers have been studied extensively for their potential use in the various fields of science[5] and have recently shown promise in creating thin films with extreme wetting behaviors.[7,17,18] Also, these nanoparticle-containing multilayers can be readily coated onto nonplanar geometries such as spherical colloidal particles and porous membranes.[8,13,19−21]

Although researchers in this field have generally shown that multilayer thin films comprising nanoparticles and oppositely charged polyelectrolytes can be readily prepared, only a few studies have shown that multilayers of oppositely charged nanoparticles can be assembled.[22,23] It is interesting to note, however, that the very first report of the preparation

* Corresponding author. E-mail: recohen@mit.edu (R.E.C.); rubner@mit.edu (M.F.R.).
[†] Department of Chemical Engineering, Massachusetts Institute of Technology.
[‡] Department of Materials Science and Engineering and Center for Materials Science and Engineering, Massachusetts Institute of Technology.

(1) Fendler, J. H. *Nanoparticles and Nanostructured Films: Preparation, Characterization and Applications*; Wiley-VCH Verlag GmbH: Weinheim, Germany, 1998.
(2) Alivisatos, A. P. *Science* **1996**, *271*, 933−937.
(3) Hyeon, T. *Chem. Commun.* **2003**, 927−934.
(4) Pellegrino, T.; Kudera, S.; Liedl, T.; Javier, A. M.; Manna, L.; Parak, W. J. *Small* **2005**, *1*, 48−63.
(5) Decher, G.; Schlenoff, J. B., Eds. *Multilayer Thin Films: Sequential Assembly of Nanocomposite Materials*; Wiley-VCH Verlag GmbH & Co.: Weinheim, Germany, 2003.
(6) Lvov, Y.; Ariga, K.; Onda, M.; Ichinose, I.; Kunitake, T. *Langmuir* **1997**, *13*, 6195−6203.
(7) Cebeci, F. C.; Wu, Z. Z.; Zhai, L.; Cohen, R. E.; Rubner, M. F. *Langmuir* **2006**, *22*, 2856−2862.
(8) Caruso, R. A.; Susha, A.; Caruso, F. *Chem. Mater.* **2001**, *13*, 400−409.
(9) Ai, H.; Jones, S. A.; Lvov, Y. M. *Cell Biochem. Biophys.* **2003**, *39*, 23−43.
(10) Cant, N. E.; Zhang, H. L.; Critchley, K.; Mykhalyk, T. A.; Davies, G. R.; Evans, S. D. *J. Phys. Chem. B* **2003**, *107*, 13557−13562.
(11) Liang, Z. Q.; Dzienis, K. L.; Xu, J.; Wang, Q. *Adv. Funct. Mater.* **2006**, *16*, 542−548.
(12) Krasteva, N.; Besnard, I.; Guse, B.; Bauer, R. E.; Mullen, K.; Yasuda, A.; Vossmeyer, T. *Nano Lett.* **2002**, *2*, 551−555.
(13) Lu, Z. H.; Prouty, M. D.; Guo, Z. H.; Golub, V. O.; Kumar, C. S. S. R.; Lvov, Y. M. *Langmuir* **2005**, *21*, 2042−2050.
(14) Ostrander, J. W.; Mamedov, A. A.; Kotov, N. A. *J. Am. Chem. Soc.* **2001**, *123*, 1101−1110.
(15) Rouse, J. H.; Ferguson, G. S. *J. Am. Chem. Soc.* **2003**, *125*, 15529−15536.
(16) Liz-Marzan, L. M.; Mulvaney, P. *J. Phys. Chem. B* **2003**, *107*, 7312−7326.
(17) Kommireddy, D. S.; Patel, A. A.; Shutava, T. G.; Mills, D. K.; Lvov, Y. M. *J. Nanosci. Nanotechnol.* **2005**, *5*, 1081−1087.
(18) Zhai, L.; Cebeci, F. C.; Cohen, R. E.; Rubner, M. F. *Nano Lett.* **2004**, *4*, 1349−1353.
(19) Donath, E.; Sukhorukov, G. B.; Caruso, F.; Davis, S. A.; Möhwald, H. *Angew. Chem., Int. Ed.* **1998**, *37*, 2202−2205.
(20) Lee, D.; Nolte, A. J.; Kunz, A. L.; Rubner, M. F.; Cohen, R. E. *J. Am. Chem. Soc.* **2006**, *128*, 8521−8529.
(21) Hollman, A. M.; Bhattacharyya, D. *Langmuir* **2004**, *20*, 5418−5424.
(22) Kumar, A.; Mandale, A. B.; Sastry, M. *Langmuir* **2000**, *16*, 6921−6926.

10.1021/cm070111y CCC: $37.00
Published on Web 02/21/2007

of multilayers involved the layer-by-layer (LbL) deposition of oppositely charged nanoparticles without any organic processing agents.[24] This pioneering work did not receive substantial follow-up attention because the robust assembly conditions were not easily achieved for the commonly available nanoparticle systems. Thus, researchers turned their attention to the more readily processed polyelectrolyte containing multilayer systems.[5] Recently, we have re-examined the possibility of using the LbL technique in the absence of any polymer components and demonstrated that all-nanoparticle thin film coatings comprising positively charged TiO_2 nanoparticles and negatively charged SiO_2 nanoparticles can be readily assembled.[25] These all-nanoparticle multilayer coatings exhibited potentially useful antifogging, antireflection, and self-cleaning properties. The ability to tune various film characteristics, such as chemical composition, would enable the fabrication of functional coatings for specific applications. For example, others have shown that the amount of TiO_2 nanoparticles in various nanocomposite thin films is crucial in determining their photocatalytic or superhydrophilic properties.[26,27] In this respect, a comprehensive understanding of the effect of assembly conditions on the chemical composition would provide an important blueprint for the fabrication of functional thin films with desirable properties.

Iler in his seminal report describing multilayers of oppositely charged colloidal particles noted that "adsorption of colloidal silica onto positively charged alumina-coated glass substrates was most rapid and complete in the low pH range of 2 to 4".[24] Although a quantitative study on the effect of assembly conditions (i.e., pH of each nanoparticle suspension) was not performed at the time, he clearly noticed that the pH of colloidal particle suspensions had an enormous influence on the deposition characteristics of multilayers. In this study, we show that average incremental bilayer thickness, refractive index, chemical composition, and porosity of all-nanoparticle multilayer thin films comprising TiO_2 and SiO_2 nanoparticles can be varied by changing the pH of the nanoparticle suspensions. By independently changing the pH of each nanoparticle suspension, the average bilayer thickness[28] of all-nanoparticle thin films could be varied between a few nanometers to tens of nanometers. It will also be demonstrated that the chemical composition as well as the porosity of the all-nanoparticle thin films are dependent on the assembly conditions. Zeta-potential measurements of polystyrene microspheres coated with TiO_2 and SiO_2 nanoparticles show that conditions that enable complete charge reversal after the deposition of each nanoparticle layer are essential to create thick all-nanoparticle multilayers. Incomplete charge reversal leads to sparse nanoparticle adsorption at each deposition step, resulting in a relatively small incremental thickness per bilayer.

Experimental Section

Materials. Anatase titanium oxide nanoparticles STS-100 (18 wt % TiO_2 suspension in water, average particle size 7 nm, and specific surface area 320 m^2/g) were generously provided by Ishihara Sangyo Kaisha, Ltd (Japan). Silica nanoparticles Ludox TM-40 (40 wt % SiO_2 suspension in water, average particle size 22 nm, and specific surface area 140 m^2/g) were purchased from Sigma-Aldrich (St. Louis, MO). The average size of nanoparticles was provided by the suppliers.[29] Glass slides were purchased from VWR International, and 1.5 μm poly(styrene) (PS) microspheres were purchased from Polysciences, Inc.

Assembly of TiO_2/SiO_2 Nanoparticle Multilayers. Sequential adsorption of TiO_2 and SiO_2 nanoparticles onto glass substrates was performed using an automated dipping machine. The concentration of each nanoparticle suspension was adjusted to 0.03 wt %. The pH of each nanoparticle suspension was adjusted using 1.0 M HCl or NaOH. Glass substrates were degreased with 2 vol % detergent solution and then cleaned with 1.0 M NaOH solutions under sonication for 15 min. Deionized water (>18 MΩ m, Millipore Milli-Q (MQ)) was used to make the nanoparticle suspensions. The dipping time in each nanoparticle solution was 10 min followed by three rinse steps (2, 1, and 1 min) in deionized water. The pH of the nanoparticle suspensions was readjusted after deposition of every three bilayers corresponding to approximately 1.5 h. A Barnstead Thermolyne 47900 furnace was used to calcinate the films at 550 °C for 2 h.

Characterization. Thicknesses of the TiO_2/SiO_2 nanoparticle-based multilayers assembled on glass substrates were determined using a Woolham Co. VASE spectroscopic ellipsometer; the data analysis was done using the WVASE32 software package. An uncoated glass slide was first scanned in the ellipsometer. Measurements were performed from 300 to 900 nm at an angle of incidence of 70°. The data obtained were fitted to a Cauchy model, which assumes that the real part of the refractive index (n_f) can be described by

$$n_f(\lambda) = A_n + \frac{B_n}{\lambda^2} + \frac{C_n}{\lambda^4} \quad (1)$$

where A_n, B_n, and C_n are constants and λ is the wavelength of the light. The values of the refractive index reported in this study were determined at 633 nm.

The zeta-potential and hydrodynamic diameter of the each nanoparticle (or aggregates of nanoparticles) as a function of pH were determined using a ZetaPals (Brookhaven Instrument Corp.) and a 90Plus Particle Size Analyzer (Brookhaven Instrument Corp.), respectively. Measurements were made within 1 h of pH adjustments.

For measurement of zeta-potential after each deposition step, TiO_2/SiO_2 multilayers were assembled onto polystyrene (PS) microspheres whose diameter was 1.5 μm. To facilitate the adsorption of nanoparticles, we primed PS microspheres with five

(23) Hao, E. C.; Yang, B.; Zhang, J. H.; Zhang, X.; Sun, J. Q.; Shen, S. C. *J. Mater. Chem.* **1998**, *8*, 1327−1328.
(24) Iler, R. K. *J. Colloid Interface Sci.* **1966**, *21*, 569−594.
(25) Lee, D.; Rubner, M. F.; Cohen, R. E. *Nano Lett.* **2006**, *6*, 2305−2312.
(26) Nakajima, A.; Hashimoto, K.; Watanabe, T.; Takai, K.; Yamauchi, G.; Fujishima, A. *Langmuir* **2000**, *16*, 7044−7047.
(27) Machida, M.; Norimoto, K.; Watanabe, T.; Hashimoto, K.; Fujishima, A. *J. Mater. Sci.* **1999**, *34*, 2569−2574.
(28) The term "average bilayer thickness" is used to represent the incremental thickness measured after a sequential exposure of substrates to TiO_2 and SiO_2 nanoparticle suspensions. The term "bilayer" in this sense is not meant to indicate that one dense layer of SiO_2 nanoparticles is formed on top of a single layer of TiO_2 nanoparticles.

(29) Average particle sizes of SiO_2 and TiO_2 nanoparticles determined by dynamic light scattering were 24.2 ± 4.2 and 8.7 ± 3.2 nm, respectively. Similar values were obtained via transmission electron microscopy; that is, 24.2 ± 2.7 nm for SiO_2 and 6.5 ± 1.3 nm for TiO_2 nanoparticles. To be consistent with our previous papers (refs 7 and 25), the nominal size of each nanoparticle as indicated by the suppliers will be used in this work.

bilayers of poly(allylamine hydrochloride) (PAH) and poly(styrene sulfonate) (PSS) (the pH of each polyelectrolyte solution was ~4, and 0.1 M NaCl was added to each solution) prior to the deposition of TiO_2/SiO_2 nanoparticle multilayers. The zeta-potential of the coated microspheres after each adsorption step was measured in pH adjusted deionized water. To create hollow microcapsules of TiO_2 and SiO_2 nanoparticles, PS microspheres coated with 5 bilayers of TiO_2 and SiO_2 nanoparticles were calcinated at 550 °C for 2 h. These calcinated hollow microcapsules were observed with a JEOL 6320FV field-emission high-resolution scanning electron microscope (SEM) at an acceleration voltage of 2 kV. The samples were coated with 10 nm of Au/Pd prior to SEM observation.

The porosity and chemical composition of the multilayers were determined using a recently reported method[25] based on ellipsometry. In brief, all-nanoparticle multilayers (12 bilayers) assembled on Si substrates at different assembly conditions were first calcinated at 550 °C for 2 h. The calcination prevents the swelling of films in water. The refractive indices of the films were then measured in air ($n_{f,1}$) and in water ($n_{f,2}$) using the ellipsometer. The porosity and the chemical composition of the multilayers are then calculated by the following equations

$$p = \frac{n_{f,2} - n_{f,1}}{n_{f,water} - n_{f,air}} = \frac{n_{f,2} - n_{f,1}}{0.33} \quad (2)$$

$$v_{TiO_2} = \frac{n_{f,framework} - n_{f,SiO_2}}{n_{f,TiO_2} - n_{f,SiO_2}}(1 - p) \quad (3)$$

$$v_{SiO_2} = 1 - (p + v_{TiO_2}) \quad (4)$$

where v, p, and n_f represent the volume fraction of each nanoparticle, the porosity, and the refractive index of the nanoparticles, respectively. Framework denotes the solid materials in the multilayer thin films that consist of TiO_2 and SiO_2 nanoparticles. For detailed derivation of eqs 2−4, see ref 25. Refractive indices of the TiO_2 and SiO_2 nanoparticles were determined to be 2.29 and 1.45, respectively. The chemical composition of the multilayers is reported in weight fraction of TiO_2 nanoparticles using the density of each nanoparticle (TiO_2 = 3.9 g/cm^3 and SiO_2 = 1.3 g/cm^3).[25]

Results and Discussion

All-nanoparticle multilayer thin films comprising 7 nm TiO_2 and 22 nm SiO_2 nanoparticles were assembled onto glass or Si substrates to determine average bilayer thicknesses.[28] Figure 1 is an example of the variation in average bilayer thickness with assembly conditions. In this case, the pH of the TiO_2 nanoparticle suspension was held constant at pH 3.0, whereas that of the SiO_2 nanoparticle suspension was varied from 2.0 to 5.0 by a single pH unit. Thicknesses were measured every three bilayers up to 12 bilayers for each condition and then the average bilayer thickness was determined using linear regression. To eliminate the effect of substrates, the regression lines were drawn without forcing the fit through the origin. In all cases, the R-squared values were greater than 0.95, indicating that the multilayers assembled at all conditions showed linear growth behavior up to 12 bilayers. The fact that some of the regression lines do not go through the origin, however, indicates the existence of substrate effects in the first few bilayers of the multilayer films.

Following the procedure described above, 12 different combinations of pH conditions were used to create a matrix

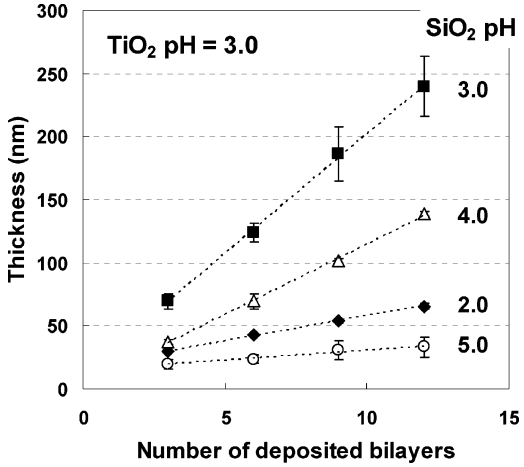

Figure 1. Increase in the thickness of TiO_2 3.0/SiO_2 *y* multilayers as a function of the number of deposited bilayers, where *y* is the pH of the SiO_2 nanoparticle suspension. The values of *y* are shown in the legend of the graph. The nanoparticle multilayer thin films were assembled on glass substrates.

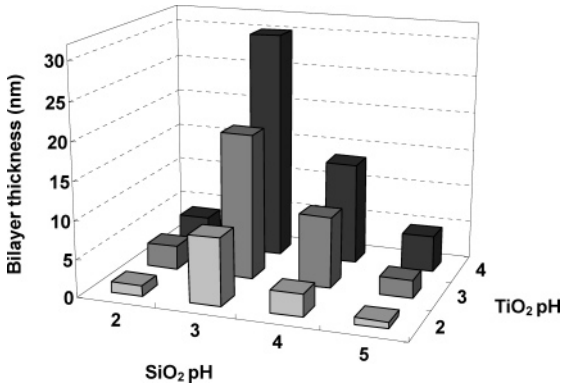

Figure 2. pH matrix showing the average bilayer thickness of 7 nm TiO_2/22 nm SiO_2 nanoparticle multilayers as a function of nanoparticle suspension pH. At least two measurements were made and averaged for each multilayer. Error in the average bilayer thickness for each multilayer is less than 2.5 nm.

of average bilayer thickness as shown in Figure 2. Depending on the assembly conditions, multilayers can show either very little growth (~2 nm/bilayer) or a large growth (~30 nm/bilayer) after a sequential exposure of substrates to TiO_2 and SiO_2 nanoparticle suspensions. Clear trends are observed as the assembly conditions are changed. For a constant pH of the SiO_2 nanoparticle suspension, the average bilayer thickness increases as the pH of the TiO_2 suspension is increased, exhibiting the greatest thickness at pH 4.0. For a constant pH of the TiO_2 nanoparticle suspension, on the other hand, the average bilayer thickness goes through a maximum at pH 3.0 for the SiO_2 nanoparticle suspensions. Iler also observed that the multilayer assembly of SiO_2 nanoparticles and positively charged colloidal particles such as alumina showed the maximum growth at pH 3.0 when the pH of the positively charged particle suspension was held constant at 4.0.[24] All multilayers shown in Figure 2 yielded completely transparent films with high uniformity. When the pH of the TiO_2 nanoparticles was increased to pH 5.0, the films became cloudy, independent of the pH of the SiO_2 suspensions. As will be described below, the opaqueness of the films assembled at pH 5.0 is likely due to the formation (and

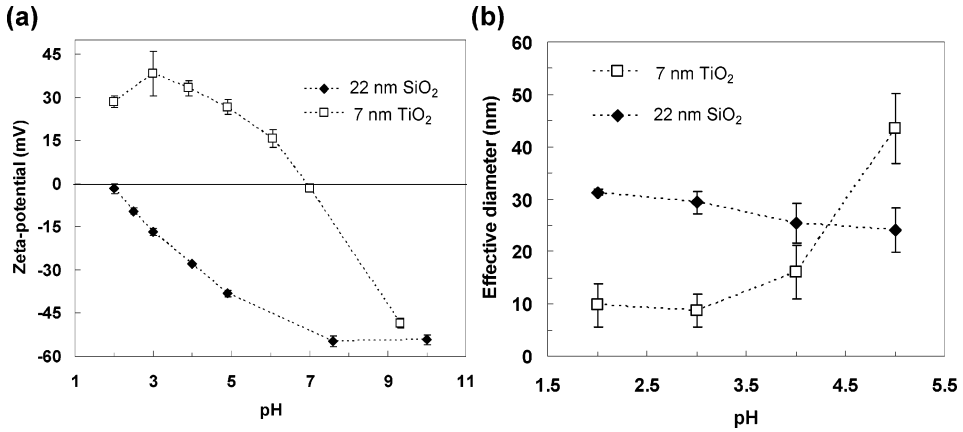

Figure 3. (a) Zeta-potential and (b) effective diameter of suspended nanoparticles determined by dynamic light scattering as a function of nanoparticle suspension pH.

adsorption) of large TiO_2 nanoparticle aggregates in the suspension.

The results obtained in Figure 2 indicate that there exists a narrow regime of pH conditions in which assembly proceeds in a "successful" layer-by-layer manner. Specifically, the average bilayer thickness observed for all conditions except the pH range between 3.0 and 4.0 for both nanoparticle suspensions is significantly less than the diameter of the SiO_2 nanoparticles themselves. Therefore, successful LbL assembly leading to significant adsorption of nanoparticles at each deposition step occurs only within this narrow assembly window. As will be shown below, the complete charge reversal of multilayers after each nanoparticle deposition step is essential for successful LbL assembly.

To better understand the effect of pH on the growth behavior of the TiO_2/SiO_2 nanoparticle multilayers, the zeta-potential and the size of nanoparticles (or that of nanoparticle aggregates) as a function of suspension pH were determined as shown in Figure 3. For SiO_2 nanoparticles, the surface charge density decreases as the pH of the suspension decreases; the isoelectric point is reached around pH 2.0. The size of the SiO_2 entities in suspension, determined by dynamic light scattering (DLS), does not vary significantly over the pH range that was used for multilayer assembly, indicating that even though the surface charge density of the SiO_2 particles changes significantly from pH 5.0 to 2.0, the particles are quite stable against flocculation. Excellent colloidal stability of SiO_2 nanoparticles near their isoelectric point has been well-documented and reported by others.[30−32] In the case of TiO_2 nanoparticles, the charge density of the nanoparticles continually decreases above pH 3.0. The TiO_2 nanoparticles used in this study exhibited an isoelectric point near pH 7.0, which is consistent with reported values for TiO_2 nanoparticles.[33−35] The observed decrease in the zeta-potential at pH 2.0 is likely due to compression of the electric double layer as the ionic strength increases at such a low pH.[36] The size of suspended TiO_2 entities, determined via DLS, increases with increasing pH, indicating that these nanoparticles flocculate into large clusters at pH values higher than 3.0. At pH 5.0, the size of the aggregates is larger than the TiO_2 nanoparticles at pH 3.0 by a factor of 5, and some precipitation of nanoparticle aggregates was observed. Our observation of a relatively low colloidal stability of TiO_2 nanoparticles compared to SiO_2 nanoparticles near the isoelectric point also has been observed by others.[34,37,38] As briefly mentioned above, the formation and adsorption of large aggregates of TiO_2 nanoparticles at pH 5.0 leads to the formation of multilayers that scatter light.[39]

Figure 3a explains the reason behind the observed negligible multilayer growth when the pH of the SiO_2 nanoparticle suspension is 2.0 regardless of TiO_2 pH (Figure 2). Because the SiO_2 nanoparticles are barely charged near their isoelectric point at pH 2.0, their electrostatic interaction with positively charged TiO_2 nanoparticles is extremely weak, leading to the negligible bilayer growth observed. It is reasonable to postulate that negligible multilayer growth would also be observed if the pH of the TiO_2 nanoparticle suspension was adjusted to 7.0; however, due to the aggregation and precipitation of TiO_2 nanoparticles above pH 5.0 (Figure 3b), this regime cannot be accessed experimentally.

The zeta-potential of TiO_2/SiO_2 nanoparticle multilayer coated polystyrene microspheres was monitored after each deposition step to provide important insight to the effect of assembly conditions on the surface charge density of multilayers during the adsorption of nanoparticles. For this purpose, two conditions were chosen: TiO_2 3.0/SiO_2 3.0 and TiO_2 3.0/SiO_2 5.0.[40] Whereas the former condition exhibited a bilayer growth of ca. 20 nm, the latter showed very limited growth of ca. 2 nm per bilayer. The comparison of these

(30) Depasse, J.; Watillon, A. *J. Colloid Interface Sci.* **1970**, *33*, 430−438.
(31) Depasse, J. *J. Colloid Interface Sci.* **1999**, *220*, 174−176.
(32) Binks, B. P.; Lumsdon, S. O. *Phys. Chem. Chem. Phys.* **1999**, *1*, 3007−3016.
(33) Mandzy, N.; Grulke, E.; Druffel, T. *Powder Technol.* **2005**, *160*, 121−126.
(34) Tkachenko, N. H.; Yaremko, Z. M.; Bellmann, C.; Soltys, M. M. *J. Colloid Interface Sci.* **2006**, *299*, 686−695.
(35) Zhao, J. C.; Hidaka, H.; Takamura, A.; Pelizzetti, E.; Serpone, N. *Langmuir* **1993**, *9*, 1646−1650.
(36) Hunter, R. J. *Zeta Potential in Colloid Science: Principles and Applications*; Academic Press: London, 1981.
(37) Imae, T.; Muto, K.; Ikeda, S. *Colloid Polym. Sci.* **1991**, *269*, 43−48.
(38) Grishchenko, L. I.; Medvedkova, N. G.; Nazarov, V. V.; Frolov, Y. G. *Colloid J.* **1994**, *56*, 215−217.
(39) Average bilayer thicknesses of (TiO_2 5.0/SiO_2 3.0) and (TiO_2 5.0/SiO_2 5.0) were determined to be ∼30 and 33 nm, respectively, as determined via ellipsometry. These films are opaque and scatter light.

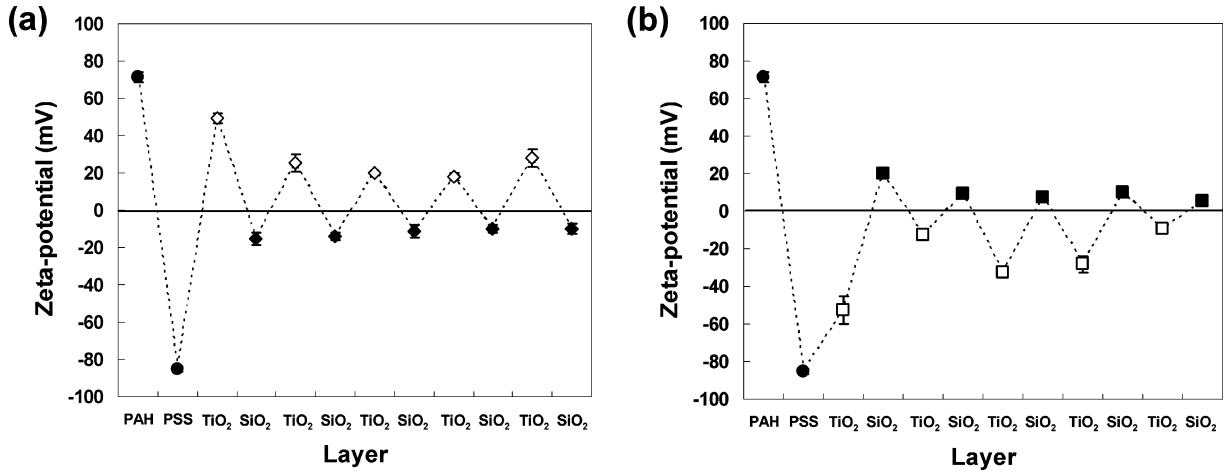

Figure 4. Zeta-potential variation of (TiO_2 3.0/SiO_2 3.0) and (TiO_2 3.0/SiO_2 5.0) multilayers deposited on 1.5 μm polystyrene (PS) microparticles. The PS particles were coated with 5 bilayers of (PAH/PSS) multilayers prior to the deposition of TiO_2/SiO_2 multilayers. Filled and open symbols in each figure represent zeta-potentials of coated PS microspheres after adsorption of SiO_2 and TiO_2 nanoparticles, respectively.

two extreme cases revealed important information regarding the dependence of layer thickness on assembly conditions. After the adsorption of each nanoparticle layer, coated PS microspheres were dispersed in deionized water whose pH was adjusted to the same value as that of the next nanoparticle suspension. For example, in the case of TiO_2 3.0/SiO_2 5.0 multilayers, after the adsorption of TiO_2 nanoparticles at pH 3.0 and three rinse steps, the coated PS microspheres were then dispersed in pH 5.0 adjusted-DI water for the measurement of zeta-potential. This scheme allowed us to probe the surface charge density at each nanoparticle deposition step and its subsequent effect on the adsorption of nanoparticles.

Figure 4a clearly shows that for TiO_2 3.0/SiO_2 3.0 multilayers, after deposition of each nanoparticle layer, the surface charge of the multilayer is completely reversed. This charge reversal leads to a complete adsorption from the next nanoparticle suspension in the processing scheme. It is a well-understood fact that charge reversal after deposition of each layer of polyelectrolyte or charged nanoparticles is essential for a successful build-up of multilayer thin films.[41−43]

In the case of the TiO_2 3.0/SiO_2 5.0 multilayers, however, each nanoparticle adsorption step does not necessarily induce charge reversal (Figure 4b). Specifically, after the deposition step of positively charged TiO_2 nanoparticles at pH 3.0, the coated-PS microspheres still exhibit a negative surface charge at pH 5.0, whereas the coated-PS microspheres have positive surface charge in pH 3.0 water after the deposition step of silica nanoparticles at pH 5.0. These results preclude any significant electrostatically driven nanoparticle adsorption in this set of processing conditions, consistent with the very low value of bilayer thickness observed at TiO_2 3.0/SiO_2 5.0 (Figure 2). We believe the major reason for the observed negligible growth of multilayers at numerous other conditions (i.e., conditions except for pH ranges between 3.0 and 4.0) observed in Figure 2 is due to the incomplete charge reversal after the deposition of each nanoparticle layer. Also, it can be concluded that a high surface charge density of suspended nanoparticles (e.g., pH 5.0 for SiO_2 nanoparticles) does not necessarily result in a large average bilayer thickness.

The observed incomplete charge reversal is likely due to the changes in the surface charge density of nanoparticles near the surface of the multilayer thin films. For example, when SiO_2 nanoparticles are adsorbed at pH 5.0, their surface charge density is relatively high, as evidenced by the zeta-potential value in Figure 2. SiO_2 nanoparticles will adsorb on top of previously adsorbed TiO_2 nanoparticles but because of the high charge density of the SiO_2 nanoparticles and low surface charge of the previously adsorbed TiO_2 nanoparticle layers, SiO_2 nanoparticles cannot adsorb into dense layers on top of the TiO_2 nanoparticle layers. When the SiO_2 nanoparticle-coated surface is exposed to a TiO_2 nanoparticle suspension at pH 3.0, the surface charge density of the outermost SiO_2 nanoparticle layer decreases and that of the underlying TiO_2 nanoparticles increases. Due to the changes in the surface charge density of nanoparticles near the surface, the multilayer exhibits positive surface charge overall, leading to little adsorption of positively charged TiO_2 nanoparticles from the suspension. Therefore, continuous exposure of the substrates to nanoparticle suspensions at this condition (i.e., TiO_2 3.0/SiO_2 5.0) leads only to the negligible growth observed in Figure 2.

The effect of assembly conditions on the growth of multilayers could be directly observed by creating hollow microcapsules of all-nanoparticle multilayers assembled at the two conditions mentioned above. Hollow microcapsules comprising TiO_2 and SiO_2 nanoparticles were obtained by calcinating the PS microspheres after the deposition of five bilayers of TiO_2 and SiO_2 nanoparticles at the two conditions. Figure 5 shows that, depending on the assembly conditions, two completely different microcapsules can be prepared. The calcinated hollow microcapsules (as evidenced by a broken capsule in the inset of Figure 5a) assembled at (TiO_2 3.0/SiO_2 3.0) show that because of the thick capsule walls, the microcapsules do not undergo the collapse that occurs during

(40) The values following TiO_2 and SiO_2 represent the pH of respective nanoparticle suspensions. For example, (TiO_2 3.0/SiO_2 5.0) represents multilayers assembled with TiO_2 and SiO_2 nanoparticle suspensions adjusted to pH 3.0 and 5.0, respectively.

(41) Netz, R. R.; Joanny, J. F. *Macromolecules* **1999**, *32*, 9013−9025.
(42) Lvov, Y.; Decher, G.; Sukhorukov, G. *Macromolecules* **1993**, *26*, 5396−5399.
(43) Abu-Sharkh, B. *Langmuir* **2006**, *22*, 3028−3034.

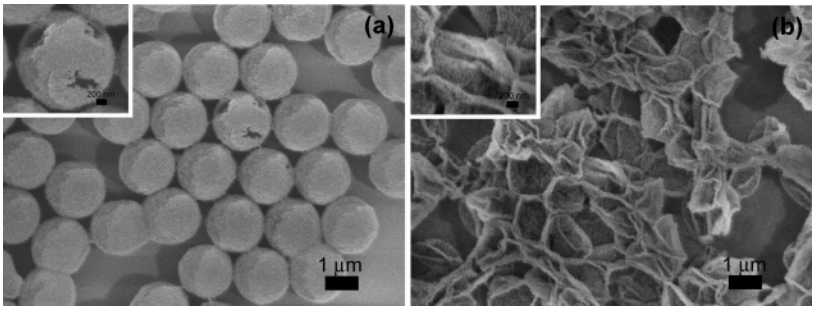

Figure 5. SEM images of (a) $(TiO_2\ 3.0/SiO_2\ 3.0)_5$ and (b) $(TiO_2\ 3.0/SiO_2\ 5.0)_5$ hollow microcapsules. Samples prepared by depositing five bilayers of TiO_2 and SiO_2 nanoparticles on top of $(PAH/PSS)_5$-coated PS microspheres were calcinated at 550 °C for 2 h. Due to the uneven evaporation of Au/Pd coatings for SEM imaging, the image on the top shows incomplete coating of Au/Pd on the TiO_2/SiO_2 hollow microcapsules. Insets show high-magnification images of hollow microcapsules.

calcination of microcapsules assembled at $(TiO_2\ 3.0/SiO_2\ 5.0)$. The collapsed microcapsules (Figure 5b) indicate that because of the incomplete charge reversal, these capsule walls are extremely thin, even after the five cycles of the deposition process. Caruso et al. have shown that inorganic hollow spheres (without structural collapse) can also be created by calcinating polystyrene microspheres coated with charged inorganic nanoparticles and an oppositely charged polyelectrolyte.[8]

All-nanoparticle thin films comprising TiO_2 and SiO_2 nanoparticles have self-cleaning properties due to the presence of TiO_2 nanoparticles. Also, these films are porous in nature because of the presence of interstitial void volume between randomly packed nanoparticles.[25] The control of the porosity of these films will enable, for example, the investigation of effect of porosity on wetting behavior or on mechanical properties[44] of these all-nanoparticle thin films. Also, the ability to control chemical composition by controlling the assembly conditions of these all-nanoparticle multilayers would offer great advantages in creating functional thin films for specific applications. For example, Nakajima et al. have shown that a precise control over the amount of TiO_2 is crucial in maintaining the long-term stability of the superhydrophobicity in self-cleaning transparent superhydrophobic thin films.[26] We have examined the effect of assembly conditions on chemical composition, porosity, and refractive index of the TiO_2/SiO_2 nanoparticle multilayers using a method based on ellipsometry described briefly in the Experimental Section and in detail in ref 25. This method allows the determination of porosity and chemical composition without making any assumption about the refractive index of each nanoparticle.

Figure 6a shows that the TiO_2 content in these all-nanoparticle multilayers can be varied from 5 to 25 wt % or 2 to 10 vol % (see the Supporting Information). Within pH ranges where the average bilayer thickness is comparable to the size of the nanoparticles (i.e., pH range between 3.0 and 4.0 for both nanoparticle suspensions), the TiO_2 content could be varied from ca. 5 to 20 wt %. In general, increasing the pH of each nanoparticle suspension increased the amount of TiO_2 nanoparticles in the multilayers. An understanding of the effect of assembly conditions on chemical composition of the multilayers enables the fabrication of all-nanoparticle thin films with desirable amount of TiO_2 nanoparticles. It should be possible, for example, to create self-cleaning thin films with varying degrees of photocatalytic activities.

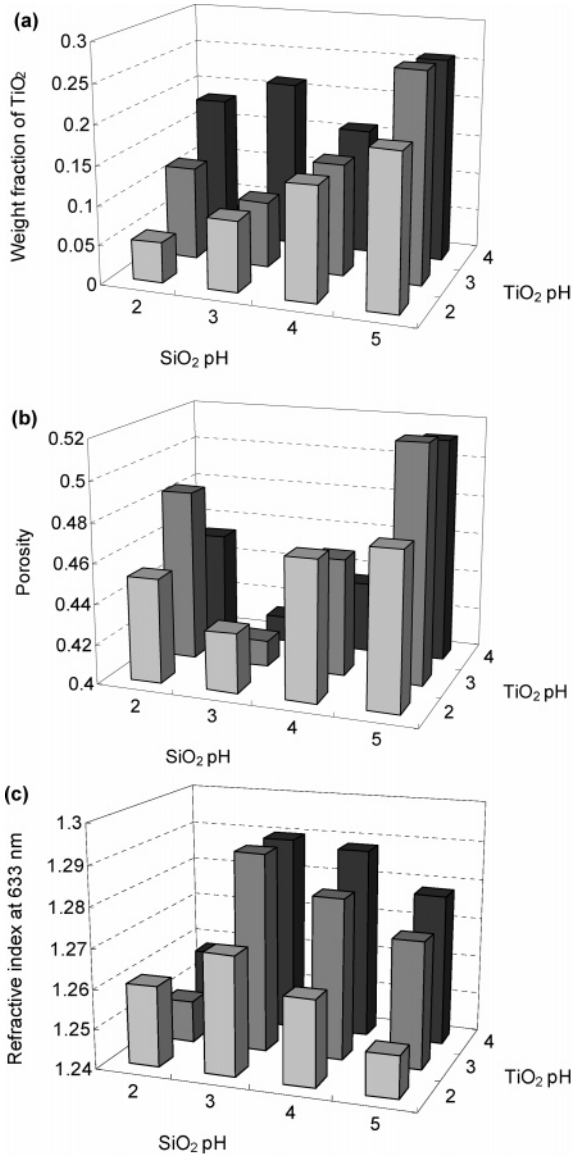

Figure 6. (a) Weight fraction of TiO_2 nanoparticles, (b) porosity, and (c) effective refractive index of the multilayers as a function of assembly pH as determined via ellipsometry. TiO_2/SiO_2 nanoparticle multilayer thin films with 12 bilayers were assembled on Si substrates for the determination of porosity and chemical composition.

(44) Stafford, C. M.; Harrison, C.; Beers, K. L.; Karim, A.; Amis, E. J.; Vanlandingham, M. R.; Kim, H. C.; Volksen, W.; Miller, R. D.; Simonyi, E. E. *Nat. Mater.* **2004**, *3*, 545−550.

The porosity of these films can also be varied as much as 10% depending on the assembly conditions, as seen in Figure 6b. It is noteworthy that the assembly pH that leads to thick bilayer growth results in lower porosity. This result indicates that the conditions that favor thick bilayer growth also favor the adsorption of densely packed nanoparticle layers. In addition to the control of assembly conditions, our previous study has shown that the use of nanoparticles of different sizes provides another approach to control the porosity of these all-nanoparticle thin films.[25]

Figure 6c shows that although changes in the refractive index of the films are observed, the difference in the refractive index between different conditions is very small (less than 0.05), even though the average bilayer thickness varies considerably (Figure 2). The lack of significant changes in the refractive index of the films can be explained by the fact that multilayer assembly conditions that lead to higher porosity, in general, result in greater volume fraction of TiO_2 nanoparticles in the multilayer thin films. As TiO_2 nanoparticles have a high refractive index of $\sim$2.3, a greater volume fraction of TiO_2 nanoparticles will offset the effect of a higher porosity; this self-compensatory behavior causes the refractive indices of the all-nanoparticle films studied here to remain essentially constant.

Conclusions

We demonstrated that by controlling the assembly conditions (i.e., pH of each nanoparticle suspension) of multilayers comprising oppositely charged TiO_2 and SiO_2 nanoparticles, it is possible to vary the average bilayer thickness of multilayers as well as the porosity and chemical composition. Changes in the zeta-potential of TiO_2/SiO_2 multilayers assembled on polystyrene microspheres at different conditions indicated that although complete charge reversal after each nanoparticle adsorption step leads to the growth of thick layers, incomplete charge reversal results in very little incremental growth. The chemical composition and porosity of these all-nanoparticles also could be varied by controlling the assembly conditions. These observations will facilitate the fabrication of all-nanoparticle thin films with characteristics to suit specific applications. The refractive index of the TiO_2/SiO_2 nanoparticles multilayers showed negligible changes within the assembly conditions employed.

Acknowledgment. This work was supported by the MIT MRSEC program of the National Science Foundation (Grant DMR 03-13282) and the DuPont−MIT Alliance (DMA). The authors thank the Center for Materials Science and Engineering (CMSE) and the Institute for Soldier Nanotechnologies (ISN) for use of their characterization facilities. D.O. was supported by the MIT CMSE−Roxbury Community College (RCC) program as a part of the MIT MRSEC program. The MIT CMSE−RCC program gratefully acknowledges support from Dr. Raymond Turner, the Executive Dean of RCC, the MIT Deans of Science and Engineering, and the MIT Vice President for Research. Ishihara Sangyo Kaisha (ISK), Ltd., generously provided the TiO_2 nanoparticles (STS-100) used in this study.

Supporting Information Available: Volume fraction of TiO_2 nanoparticles in TiO_2/SiO_2 nanoparticle multilayers as a function of assembly pH. This material is available free of charge from http://pubs.acs.org/.

CM070111Y